Proc. Natl. Acad. Sci. USA
Vol. 87, pp. 7419–7423, October 1990
Cell Biology

Vectorial apical delivery and slow endocytosis of a glycolipid-anchored fusion protein in transfected MDCK cells

(cell polarity/glycosyl-phosphatidylinositol/intracellular sorting/kidney epithelial cell)

MICHAEL P. LISANTI*, INGRID W. CARAS†, THIERRY GILBERT*, DAVID HANZEL*, AND ENRIQUE RODRIGUEZ-BOULAN*‡

*Department of Cell Biology and Anatomy, Cornell University Medical College, New York, NY 10021; and †Genentech, Inc., 460 Point San Bruno Boulevard, South San Francisco, CA 94080

Communicated by Bernard L. Horecker, June 21, 1990

ABSTRACT **To characterize the mechanisms that determine the apical polarity of proteins anchored by glycosyl-phosphatidylinositol (GPI), we studied the targeting of a GPI-anchored form of a herpes simplex glycoprotein, gD-1, in transfected MDCK cells. Using a biotin-based targeting assay, we found that GPI-anchored gD-1 was sorted intracellularly and delivered directly to the apical surface. Endocytosis of GPI-anchored gD-1 occurred slowly and preferentially from the apical domain, while transcytosis of the basolateral fraction did not occur at a significant rate (incompatible with being a precursor to the apical pool). Prevention of tight junction formation by incubation in medium with micromolar Ca^{2+} resulted in expression of GPI-anchored gD-1 on the free surface, but not on the attached surface of the cell. Our results indicate that the apical polarity of a GPI-anchored protein is generated by vectorial delivery to the apical membrane, where its distribution is maintained by slow endocytosis and by a retention system not necessarily involving the tight junction.**

The vectorial properties of epithelial cells derive from the polarized distribution of their plasma membrane proteins and lipids (1, 2). This asymmetry between apical and basolateral surfaces depends upon domain-selective surface delivery (biosynthetic and postendocytic) and retention at the appropriate domain via cytoskeletal anchorage and/or the tight junctional fence (1, 2). Sorting of newly synthesized apical proteins to their final destination can occur at two sites: intracellularly, at the trans-Golgi network (TGN) (3–5), or at the basolateral membrane (6–8). The latter route (transcytosis of apical proteins) may serve as a major biogenetic pathway (6, 7) or as a corrective pathway for the missorted basolateral fraction (7, 8).

The molecular signals that direct a protein to a given pathway are poorly understood. We (9–12) and others (13, 14) have presented evidence for the conserved apical localization of both endogenous and exogenous proteins anchored by glycosyl-phosphatidylinositol (GPI) (15–17). Direct evidence of an apical sorting role for GPI was obtained by its recombinant transfer to other proteins. GPI anchoring of two independent basolateral antigens (11, 13) or of a regulated secretory protein (11) led to apical expression in transfected Madin–Darby canine kidney (MDCK) cells (17). Although these results indicate that membrane anchoring by GPI may act as a signal for apical localization, the mechanisms by which GPI-anchored proteins attain and maintain their apical distribution remain unknown.

Here, we examine the biogenesis of a GPI-anchored protein in transfected MDCK cells. Our results indicate that vectorial apical delivery, slow endocytosis, and tight junction-independent retention determine its apical localization.

MATERIALS AND METHODS

Reagents. Cell surface labeling reagents were from Pierce. Sources for anti-herpes simplex virus (HSV) rabbit IgG (for immunoprecipitation) and anti-gD-1 monoclonal antibody (mAb) (IgG2a; for immunofluorescence) were as described (11). mAb (IgG1) to human transferrin receptor was from Boehringer Mannheim.

Cell Culture. Transfected MDCK (type II) cells expressing native gD-1 (transmembrane form) or gD-1–DAF (GPI-anchored form; DAF represents the C terminus of decay-accelerating factor; ref. 18) were maintained in Dulbecco's modified Eagle's medium (DMEM) supplemented with 10 mM Hepes (pH 7.3), 10% fetal bovine serum (FBS), nonessential amino acids, and antibiotics (normal medium) (11). Cells from a single confluent 75-cm^2 flask were trypsinized and transferred to six Transwells (Costar); 12–16 hr before the fifth day of plating, sodium butyrate (10 mM) was used to increase expression of the transfected gene products (11).

Domain-Selective Labeling. Filter-grown monolayers were washed twice with ice-cold phosphate-buffered saline containing 0.1 mM $CaCl_2$ and 1 mM $MgCl_2$ (PBS-C/M) before addition of the labeling reagent (described below). After labeling, cell monolayers were washed twice with PBS-C/M and processed for immunoprecipitation.

Steady state. Sulfosuccinimidobiotin (sulfo-NHS-biotin, 0.5 mg in 1 ml of ice-cold PBS-C/M) was added to either the apical or the basolateral compartment (9, 19). After 15 min at 4°C, the medium was removed and the labeling procedure was repeated twice. After labeling, excess reactive biotin was quenched by incubation with Hepes-buffered serum-free DMEM (10 min at 4°C). For detection of gD-1–DAF only one round of biotinylation was necessary, whereas three rounds were required for native gD-1.

Cell surface delivery. To quench free amino groups on the cell surface, sulfosuccinimidyl 3-(4-hydroxyphenyl)propionate (sulfo-SHPP, 0.5 mg in 1 ml of ice-cold PBS-C/M) was added to both the apical and basolateral compartments. Approximately 90% of reactive cell surface amino groups are quenched after only a single labeling with sulfo-SHPP (20). After 15 min at 4°C, the solution was removed and the labeling procedure was repeated five times; residual reactive sulfo-SHPP was quenched as described above for sulfo-NHS-biotin. The appearance of new free surface amino

The publication costs of this article were defrayed in part by page charge payment. This article must therefore be hereby marked "*advertisement*" in accordance with 18 U.S.C. §1734 solely to indicate this fact.

Abbreviations: GPI, glycosyl-phosphatidylinositol; DAF, decay-accelerating factor; sulfo-NHS-biotin, sulfosuccinimidobiotin; NHS-SS-biotin, sulfosuccinimidyl 2-(biotinamido)ethyl-1,3-dithiopropionate; sulfo-SHPP, sulfosuccinimidyl 3-(4-hydroxyphenyl)propionate; mAb, monoclonal antibody; TGN, trans-Golgi network; VAC, vacuolar apical compartment.

‡To whom reprint requests should be addressed.

groups during incubation at 37°C with prewarmed normal medium containing 10 mM sodium butyrate was monitored by transfer, after various times, to ice-cold PBS-C/M followed by domain-selective labeling with sulfo-NHS-biotin (as described above). MDCK cells remained viable after cell surface quenching, as they exhibited incorporation of ^{35}S-labeled amino acids, plating efficiencies, and doubling times indistinguishable from those of untreated control cells. In some experiments, cycloheximide (100 μg/ml) or tunicamycin (12 μg/ml) was added to the normal medium containing sodium butyrate. These concentrations produce complete inhibition in MDCK cells (21, 22).

Endocytosis and transcytosis. Labeling with sulfosuccinimidyl 2-(biotinamido)ethyl-1,3-dithiopropionate (NHS-SS-biotin, a reducible analog of sulfo-NHS-biotin) was performed as described above for sulfo-NHS-biotin. After labeling, cells were incubated at 37°C in prewarmed normal medium to allow endocytosis to occur. After various times, endocytosis was inhibited by transfer to ice-cold PBS-C/M and the cell surface label was stripped by reduction with glutathione (twice, 20 min each at 4°C) (23, 24). For transcytosis, glutathione stripping was performed on the side opposite biotin labeling. Under these conditions, glutathione reduction is membrane- and tight junction-impermeant (4, 5, 7).

Immunoprecipitation. We used the detergent phases of Triton X-114 extracts to ensure that proteins we detected were hydrophobic (indicating the presence of an intact GPI-anchor or transmembrane domain). Cell lysis, phase separation, and immunoprecipitation with rabbit anti-HSV antibodies or anti-DAF mAb (IA10) were as described (11). For the transferrin receptor, mAbs were prebound to rabbit anti-mouse IgG/protein A-Sepharose complexes.

Detection of Biotinylated Proteins. After NaDodSO$_4$/PAGE (10% acrylamide) and transfer to nitrocellulose, biotinylated proteins were detected by blotting with ^{125}I-streptavidin (9, 19). Autoradiographs were densitometrically scanned and relative peak areas were determined with the GS-365 data system (4, 5, 9, 10).

Fluorescence Confocal Microscopy. MDCK cells expressing gD-1–DAF (one 75-cm^2 flask) were trypsinized and transferred to six Transwell filters (11). After 90 min in normal medium, the attached cells were washed six times with serum-free spinner minimal essential medium (S-MEM) and incubated 16–20 hr in Hepes-buffered S-MEM with 10 mM sodium butyrate and 10% FBS (dialyzed to deplete calcium) to prevent cell–cell contacts (25). Filters were then washed with PBS, cut into squares, fixed, and processed for immunolabeling with a mAb (26). Samples were incubated with a fluorescein-conjugated secondary antibody to visualize bound IgG and mounted (27). Vertical optical sections were obtained with a laser scanning confocal microscope (Phoibos 1000; Sarastro, Ypsilanti, MI) and analyzed with a Personal Iris computer (Silicon Graphics, Mountain View, CA). Images were recorded with a VP3500 video printer (Seikosha, Mahwah, NJ).

RESULTS AND DISCUSSION

Polarized Apical Delivery of a GPI-Anchored Protein. To study the mechanisms of apical polarization of GPI-anchored proteins in epithelial cells, we transfected DNA encoding native and glycolipid-anchored forms of herpes simplex gD-1 into MDCK cells (11). gD-1–DAF contains 300 of the 340 amino acids of the gD-1 ectodomain fused to the C-terminal 37 amino acids of DAF that constitute its GPI-attachment signal (18). Native gD-1 is a type I transmembrane protein.

The steady-state surface distribution of these antigens was quantitated by domain-selective biotinylation/^{125}I-streptavidin blotting. Eighty-five to 95% of gD-1–DAF was apically polarized (ref. 11; Fig. 1*a*) Previous attempts to quantitate the polarity of native gD-1 by cell surface biotinylation were unsuccessful (11), since it is rapidly degraded within 1–2 hr after synthesis (unlike gD-1–DAF, which is relatively stable, with $t_{1/2} > 6$ hr). Improvements of the biotinylation procedure (see *Materials and Methods*) permitted detection of native gD-1 (Fig. 1*a*), 99% of which was localized on the basolateral domain. The presence of basolateral sorting information in the ectodomain of gD-1 (11) implies that GPI dictates the apical localization of gD-1–DAF (17). Thus, gD-1–DAF is an ideal molecule to study the apical sorting role of GPI.

To follow the surface delivery of gD-1–DAF in MDCK cells, a biotin-based targeting assay was developed. Free surface amino groups were quenched at 4°C with sulfo-SHPP (a water-soluble Bolton–Hunter reagent, which lacks a biotin moiety) and the insertion of protected intracellular amino groups at the cell surface after incubation at 37°C was detected by domain-selective biotinylation and streptavidin blotting. Identical results were obtained when sulfosuccinimidyl acetate was used instead of sulfo-SHPP.

With this assay system, the surface appearance of gD-1–DAF was time- and temperature-dependent (undetectable at 4°C; rapid at 37°C) and apically polarized (Fig. 1 *b* and *c*). Apical gD-1–DAF was detected as early as 20 min after transfer to 37°C and continued to increase linearly at a rate 5–6 times the rate of basolateral appearance, without reaching a plateau. Similar results were obtained for GPI-anchored native DAF expressed in MDCK cells (data not shown). These results are consistent with intracellular sorting and vectorial apical delivery of GPI-anchored proteins. In contrast, vectorial basolateral delivery was observed for native gD-1 (data not shown), as previously observed for other basolateral proteins in various epithelial systems (1, 2, 6).

Cell Surface Delivery Derives Primarily from the Secretory Pathway. To evaluate the contribution of presynthesized and newly synthesized protein pools to cell surface delivery, protein synthesis was blocked at time 0 by addition of cycloheximide. Since the effects of this drug are practically

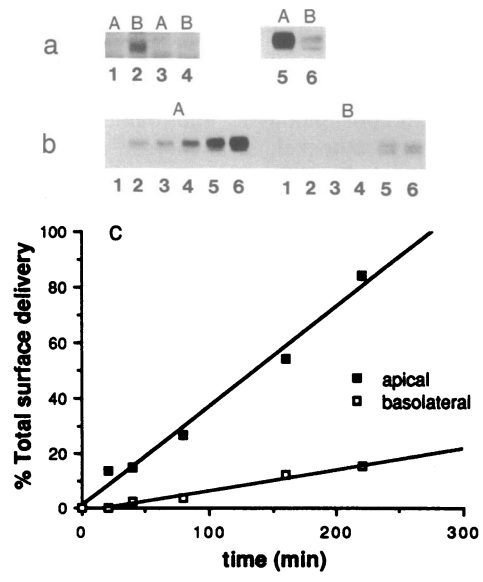

FIG. 1. Polarized apical surface delivery of gD-1–DAF. (*a*) Steady-state distribution of native gD-1 or gD-1–DAF expressed in transfected MDCK cells, determined by domain-selective biotinylation [apical (A) or basolateral (B)], immunoprecipitation, and ^{125}I-streptavidin blotting/autoradiography. Lanes: 1 and 2, gD-1-expressing cells; 3 and 4, nonexpressing MDCK cell control; 5 and 6, gD-1–DAF-expressing cells. (*b*) Arrival of intracellular gD-1–DAF at the cell surface. After surface amino groups were quenched, cells were warmed to 37°C for various times and subjected to apical (A) or basolateral (B) biotinylation. Lanes 1–6: 0, 20, 40, 80, 160, and 220 min. "Splitting" of the band corresponding to gD-1–DAF was caused by unlabeled comigrating IgG heavy chain used for immunoprecipitation. (*c*) Graphical representation of *b*.

instantaneous (>90% inhibition of protein synthesis in <3 min; ref. 21), only presynthesized protein pools in the secondary pathway or in postendocytic compartments may be delivered in the presence of cycloheximide.

Apical surface delivery of presynthesized gD-1–DAF reached maximal levels after only 40 min of incubation at 37°C, whereas basolateral surface delivery plateaued somewhat later, by 80–160 min (Fig. 2*a*). Thus, the continual cell surface delivery of gD-1–DAF observed in the absence of cycloheximide was dependent on the steady provision of newly synthesized protein. From delivery profiles of the presynthesized pool, we estimated the half-times for transport to the cell surface. gD-1–DAF was delivered faster to the apical surface ($t_{1/2}$ = 20–30 min) than to the basolateral surface ($t_{1/2}$ = 40–80 min). The rate of cell surface transport of one other GPI-anchored protein, the variable surface glycoprotein (VSG) of *Trypanosoma brucei*, has been measured (28) and is compatible ($t_{1/2}$ = 15 min) with the rate we observed for apical transport.

To dissect further the presynthesized pool of gD-1–DAF into secretory and postendocytic (recycling) components, surface delivery was studied in monolayers that were preincubated with cycloheximide for 90 min (time chosen on the basis of delivery profiles of the presynthesized pool; Fig. 2*a*). This treatment should empty the secretory pathway and leave the recycling pool unaffected. Two extreme scenarios were envisioned. If the amount of gD-1–DAF present in the secretory pathway were much larger than the amount in a recycling (endosomal) compartment, pretreatment with cycloheximide would markedly decrease cell surface delivery (as compared with untreated controls that received cycloheximide only at time 0). In the reverse scenario (amount of gD-1–DAF much larger in a postendocytic compartment than in the secretory pathway), cycloheximide pretreatment would decrease surface delivery only slightly.

Our results are compatible with the first scenario. Cycloheximide pretreatment decreased surface delivery of gD-1–DAF by ≈85% at 20 min (data not shown) and by ≈95% at 40 min (Fig. 2*b*). The small amount (5–15%) of apical delivery resistant to cycloheximide pretreatment most likely originated

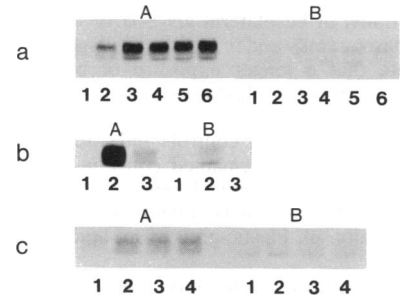

FIG. 2. Cell surface delivery of gD-1–DAF derives mainly from the secretory pathway. (*a*) Continual cell surface delivery of gD-1–DAF depends on newly synthesized protein. After quenching of surface amino groups, cells were warmed to 37°C in the presence of cycloheximide for various times and subjected to apical (A) or basolateral (B) biotinylation. Lanes 1–6: 0, 20, 40, 80, 160, and 220 min, respectively. (*b*) Cell surface delivery represents mainly newly synthesized protein. Cells were either preincubated with cycloheximide for 90 min (lane 3) or left untreated (lanes 1 and 2). Cell surface amino groups were quenched, and cells were warmed in the presence of cycloheximide for 0 min (lane 1) or 40 min (lanes 2 and 3). Intracellular gD-1–DAF reaching the apical (A) or the basolateral (B) cell surface was detected by domain-selective biotinylation. (*c*) Cell surface delivery of the cycloheximide-resistant pool. Cells were preincubated with cycloheximide for 90 min and then were warmed in the presence of cycloheximide. gD-1–DAF reaching the apical (A) or the basolateral (B) cell surface was detected by domain-selective biotinylation. Lanes 1–4: 0, 20, 160, and 220 min, respectively.

from an apical recycling pool fed by slow endocytosis from the apical surface (see below). Further, such apical delivery reached maximal levels by 20 min and did not increase over 220 min of incubation (Fig. 2, compare *c* with *a*).

Rapid Apical Delivery of gD-1–DAF After 20°C Temperature Block. At 20°C, transport between the TGN and the cell surface is blocked, but protein synthesis, glycosylation, and endoplasmic reticulum-to-Golgi transport proceed such that the TGN increases up to 5 times its normal volume (after 2 hr at 20°C); endocytosis and recycling proceed but at a slower rate (29). Similarly, low temperature (15–20°C) reduces the rate of cell surface transport of a GPI-anchored protein in trypanosomes by a factor of 4, but the transfer of GPI to newly synthesized proteins continues (28).

Monolayers were preincubated for 2 hr at 20°C and for an additional 30 min at 20°C in the presence of cycloheximide. With these preincubation conditions, surface appearance of gD-1–DAF was observed as early as 5 min, indicating that gD-1–DAF accumulated intracellularly in a compartment kinetically close to the cell surface (most likely the TGN) (Fig. 3*a*). The rate of apical delivery was 10–11 times the rate of basolateral delivery, with ≈1.75 times more protein delivered by 20 min (as compared with untreated controls). Such rapid apical delivery makes it highly unlikely that gD-1–DAF transiently passes through the basolateral membrane en route to the apical surface. However, to examine this possibility directly, we determined the fate of the basolateral fraction of gD-1–DAF (see below).

N-Glycosylation Is Not Required for Polarized Apical Delivery of gD-1–DAF. We used tunicamycin treatment to study the effect of inhibiting N-glycosylation on the polarized delivery of gD-1–DAF and as an additional approach to characterize the presynthesized pool of this protein. Inhibition of N-glycosylation does not affect the polarized distribution of viral glycoproteins in infected MDCK cells (30) but disrupts the polarized release of a major endogenous secretory protein (22).

Monolayers were either preincubated with tunicamycin (60 min) or left untreated; tunicamycin was also included during warming for pretreated cells. A downward shift in the mobility of both apically and basolaterally delivered gD-1–DAF was observed as compared with untreated controls (Fig. 3*b*). Practically all of the protein was affected by the treatment, confirming that cell surface delivery of gD-1–DAF derives primarily from the secretory pathway. Cell surface delivery increased continually, indicating that tunicamycin treatment did not prevent the synthesis or transport of gD-1–DAF (Fig. 3*b*). Delivery was ≈85% apical (identical to that in untreated monolayers processed in parallel), indicating that N-glycosylation was not necessary for the correct sorting of this GPI-anchored protein. This is consistent with our recent observation (10) that the apical polarity of four endogenous GPI-anchored proteins is preserved in a mutant MDCK cell line with a pleotropic defect in galactosylation (which results in severely truncated N- and O-linked oligosaccharide chains). Surprisingly, 2.2–2.4 times more gD-1–DAF was delivered by 180 min in tunicamycin-treated cells, suggesting that the rate of GPI biosynthesis or attachment is enhanced by inhibition of N-glycosylation.

Endocytosis and Transcytosis of gD-1–DAF Occur at a Slow or Insignificant Rate. To evaluate the contribution of the basolateral membrane as a sorting site for a GPI-anchored proteins, we studied the fate of basolateral pool of gD-1–DAF. Since following the transcytotic routes requires endocytosis (see Introduction), we first studied the kinetics of gD-1–DAF endocytosis in MDCK cells grown on plastic dishes. Cells were surface-labeled with a reducible analog of sulfo-NHS-biotin (NHS-SS-biotin) and warmed to 37°C to allow endocytosis to occur. After 0–60 min, the remaining surface label was removed by cell surface reduction with

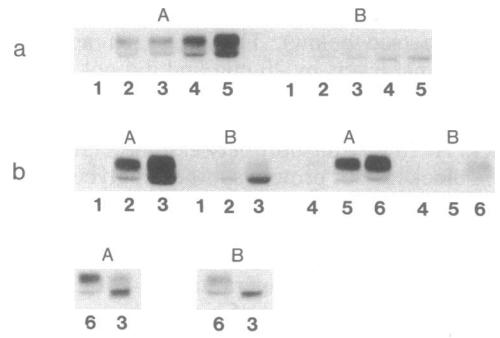

FIG. 3. Apical surface delivery of gD-1–DAF is affected by 20°C temperature block or tunicamycin. (*a*) Cells were preincubated for 2 hr at 20°C to allow the intracellular accumulation of gD-1–DAF, and then incubated for 0.5 hr at 20°C in the presence of cycloheximide to inhibit the transfer of newly synthesized proteins from the endoplasmic reticulum to the Golgi compartment. Cell surface amino groups were quenched and cells were warmed to 37°C in the presence of cycloheximide. After various times, cells were subjected to domain-selective biotinylation (A, apical; B, basolateral). Lanes 1–5: 0, 5, 10, 20, and 40 min, respectively. (*b*) Cells were preincubated with tunicamycin (lanes 1–3) for 1 hr to deplete the existing pool of dolichol-*PP*-oligosaccharides. Cell surface amino groups were quenched and cells were warmed in the presence of tunicamycin. After various times, cells were subjected to domain-selective biotinylation (A, apical; B, basolateral). Untreated control monolayers were processed in parallel for comparison (lanes 4–6). Lanes 1–3 and 4–6 represent 0, 60, and 180 min of incubation, respectively. Samples without (lane 6) or with (lane 3) tunicamycin preincubation were also run adjacently for more direct comparison of glycosylated and underglycosylated forms; adjacently run basolateral samples are shown at a longer exposure for better illustration.

glutathione, leaving only endocytosed material protected (23, 24). We observed a slow but significant rate of endocytosis; 8–10% of the total cell surface label was protected after 30–60 min (Fig. 4 *a* and *c*). Similar results were obtained with native DAF endogenously expressed in HeLa cells, whereas the transferrin receptor was rapidly endocytosed (80% in 5 min) (Fig. 4 *a* and *c*).

Polarized endocytosis or transcytosis of the basolateral fraction of gD-1–DAF was studied by sequential domain-selective labeling with NHS-SS-biotin and domain-selective reduction with glutathione. We observed that ≈38% of apically biotinylated gD-1–DAF became protected (from apical glutathione) after 120 min, whereas 2–3% of the basolaterally biotinylated fraction was protected (from basolateral glutathione) during the same time period (Fig. 4 *b* and *c*). Preferred apical endocytosis may reflect the different lipid compositions of the apical and basolateral membranes, as the apical membrane is enriched in the glycosphingolipids and depleted of phosphatidylcholine (31). As endocytosis of the entire cell surface (either apical or basolateral) requires only 120–150 min (32), apical and basolateral gD-1–DAF were endocyosed at rates 2.5 times and 33–50 times slower than constitutive internalization of the plasma membrane, respectively. Furthermore, slow apical endocytosis of gD-1–DAF may give rise to postendocytic recycling, possibly explaining the apical delivery observed after cycloheximide preincubation (see Fig. 2 *b* and *c*).

In accordance with the very slow basolateral endocytosis of gD-1–DAF, transcytosis of basolateral gD-1–DAF (measured as the fraction that became accessible to apical glutathione) was undetectable after 120 min (Fig. 4*b*). Thus, basolateral gD-1–DAF behaved as a stable missorted antigen rather than as an apical precursor pool. Since apical surface delivery of gD-1–DAF occurs rapidly, it is unlikely that the transcytotic route determines the steady-state distribution of this antigen.

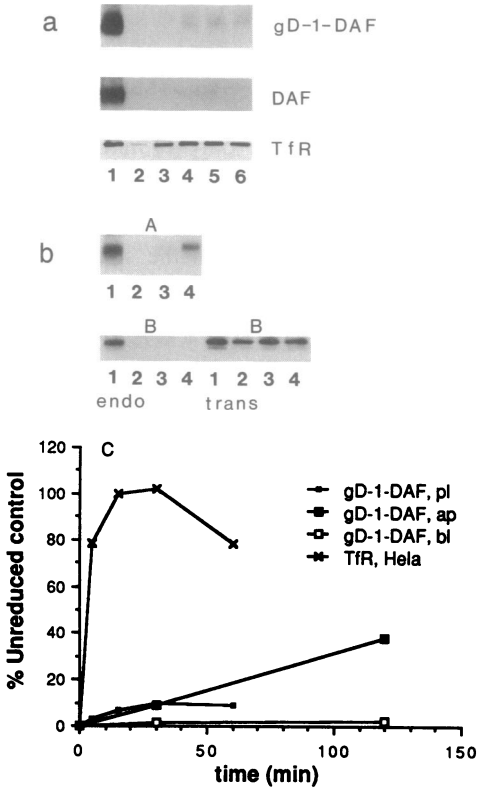

FIG. 4. Polarized endocytosis and transcytosis of gD-1–DAF. (*a*) Plastic-grown gD-1–DAF-expressing cells were surface-labeled at 4°C with NHS-SS-biotin and warmed to 37°C to allow endocytosis to occur. After various times, endocytosis was inhibited by cooling to 4°C and the remaining cell surface label was removed by glutathione reduction. Protection indicates that endocytosis of a given antigen occurs. Endocytosis of DAF and the transferrin receptor (TfR), endogenously expressed in HeLa cells, is also shown. Lanes 1–6: 0, 0, 5, 15, 30, and 60 min, respectively. Lane 1: unreduced control. Lanes 2–6: glutathione reduced. (*b*) gD-1–DAF-expressing cells, grown on Transwells, were either apically (A) or basolaterally (B) labeled at 4°C with NHS-SS-biotin and warmed to 37°C to allow endocytosis (endo) to occur and processed as described in *a*. When transcytosis (trans) of basolateral gD-1–DAF was measured, cells were labeled basolaterally and reduced apically after various times of warming. Note that a longer exposure of basolaterally labeled samples is shown for better illustration. Lanes 1–4: 0, 0, 30, and 120 min, respectively. Lane 1: unreduced control. Lanes 2–4: glutathione-reduced. Additional controls indicated that the level of surface labeled gD-1–DAF remained constant over the course of incubation at 37°C. (*c*) Graphical representation of endocytosis shown in *a* and *b*. For simplicity, results with native DAF are not depicted graphically. pl, Plastic-grown; ap, apical; bl, basolateral.

Immunolocalization studies have shown that several GPI-anchored proteins are excluded from clathrin-coated pits (Thy-1, 5′-nucleotidase, and folate receptor; reviewed in ref. 16). However, both 5′nucleotidase and folate receptors undergo endocytosis slowly (via a clathrin-independent pathway; i.e., caveolae), reaching steady state at 60–90 min with label equally distributed between the cell surface and an intracellular compartment (16, 33). These data, in addition to the observations reported here, are consistent with the current "dogma" that rapid internalization requires a signal in the cytoplasmic domain (16).

gD-1–DAF Polarizes to the Free Surface in the Absence of Cell–Cell Contact. To evaluate the role of the tight junctional fence in maintaining the asymmetric distribution of a GPI-anchored protein, we examined the polarity of gD-1–DAF in MDCK monolayers prevented from establishing cell–cell contacts and tight junctions by incubation with low Ca^{2+} (5 μM) for 16–20 hr. Under these conditions, a portion of the

apical surface is stored intracellularly as large vacuoles (vacuolar apical compartment, VAC; ref. 1). The distribution of gD-1–DAF was examined by laser scanning confocal microscopy in these monolayers, as well as in monolayers confluent in medium with normal (1.8 mM) Ca^{2+} for 1 or 5 days. In contact-free monolayers, gD-1–DAF was polarized to the free cell surface and was also detected in intracellular VACs (Fig. 5 *A* and *B*), as are other apical antigens (reviewed in ref. 1). Cells containing VACs expressed lower surface levels of gD-1–DAF, as it was retained intracellularly. Furthermore, in confluent cells gD-1–DAF did not pass from the apical surface of a high expressing cell to a nonexpressing cell (Fig. 5 *C* and *D*), confirming that the apical membranes of adjacent epithelial cells are not continuous (34).

The observation that gD-1–DAF is polarized in the absence of cell–cell contacts indicates that tight junctions (which physically define the boundary between apical and basolateral domains) may play only a secondary role in maintaining its asymmetric distribution. Other mechanisms (e.g., interaction with other apical proteins anchored to the underlying submembrane cytoskeleton, or an as yet undefined alternative "fencing" mechanism) may contribute to the apical polarization of gD-1–DAF in contact-free monolayers. These results are at variance with the described role of tight junctions in maintaining the asymmetric distribution of fluorescent lipid probes artificially implanted in the exoplasmic leaflet of the apical membrane (31). Thus, cell surface gD-1–DAF behaved more like other apical antigens than as a lipid probe, suggesting a role for a GPI recognition mechanism in the maintenance of surface polarity.

Conclusions and Significance. We have presented several lines of evidence that gD-1–DAF is recognized intracellularly as an apical antigen: (*i*) it is sorted before reaching the apical surface (independently of N-glycosylation), without transient expression on the basolateral membrane; (*ii*) it accumulates intracellularly at 20°C in a compartment kinetically close (5 min) to the apical surface; (*iii*) it undergoes a small but significant amount of apical postendocytic recycling; and (*iv*) it accumulates intracellularly in an apical post-Golgi compartment (i.e., VAC) in the presence of micromolar Ca^{2+}. As its protein ectodomain contains basolateral sorting information (11), its intracellular recognition as an apical antigen may depend on its anchoring via GPI. These and previous results suggest that the GPI-anchoring mechanism may represent the first well-defined apical transport signal for the post-Golgi sorting of plasma membrane proteins in polarized epithelial cells. As both GPI-anchored proteins (33) and glycosphingolipids (35) cluster in specialized cell surface membrane invaginations (caveolae), perhaps a similar lateral segregation mechanism operates intracellularly in the apical routing of GPI-linked proteins.

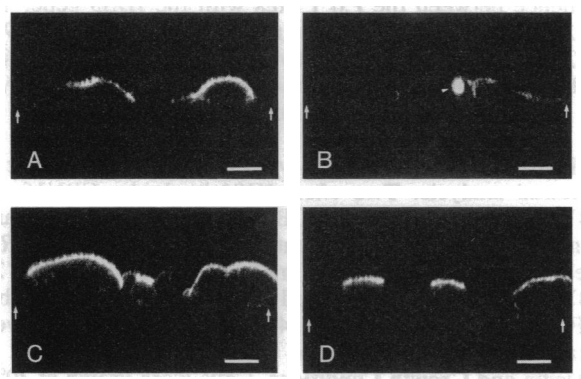

FIG. 5. gD-1–DAF is polarized to the free surface in the absence of cell–cell contact. Cells were allowed to attach for 90 min in normal-Ca^{2+} medium and then incubated for 16–20 hr in low-Ca^{2+} medium to prevent the formation of cell contacts (*A* and *B*). Control monolayers incubated in normal-Ca^{2+} medium for 16–20 hr (*C*) or 5 days (*D*) are shown for comparison. gD-1–DAF was detected using a specific mAb and the appropriate fluorescein-conjugated secondary antibody. Cells were examined with a laser scanning confocal microscope. Vertical optical sections perpendicular to the monolayer are shown; arrows point at the attached or basal surface. In low-Ca^{2+} medium, gD-1–DAF was located either on the free surface (*A*) or stored intracellularly in a VAC (*B*, arrowhead). In contrast, the development of the full apical polarity of gD-1–DAF was observed in normal medium (*C* and *D*). (Bar = 10 μm.)

We thank Michael A. Davitz (New York University) for his generous gift of anti-DAF antibodies. M.P.L. is supported by a Medical Scientist Training Grant from Cornell University; I.W.C. by Genentech, Inc.; T.G. by a fellowship from the Association pour la Recherche sur le Cancer (France); D.H. by a fellowship from the American Heart Association; and E.R.-B. by grants from the National Institutes of Health (GM34107 and GM41771), the American Cancer Society, and the American Heart Association.

1. Rodriguez-Boulan, E. & Nelson, W. J. (1989) *Science* **245,** 718–725.
2. Wandiger-Ness, A. & Simons, K. (1990) in *Intracellular Trafficking of Proteins*, eds. Hanover, J. & Steer, C. (Cambridge Univ. Press, New York), in press.
3. Lisanti, M. P., Le Bivic, A., Sargiacomo, M. & Rodriguez-Boulan, E. (1989) *J. Cell Biol.* **109,** 2117–2127.
4. Le Bivic, A., Real, F. & Rodriguez-Boulan, E. (1989) *Proc. Natl. Acad. Sci. USA* **86,** 9313–9317.
5. Le Bivic, A., Sambuy, Y., Mostov, K. & Rodriguez-Boulan, E. (1990) *J. Cell Biol.* **110,** 1533–1539.
6. Bartles, J. R. & Hubbard, A. L. (1988) *Trends Biochem. Sci.* **13,** 181–184.
7. Le Bivic, A., Quaroni, A., Nichols, B. & Rodriguez-Boulan, E. (1990) *J. Cell Biol.*, in press.
8. Matter, K., Brauchbar, M., Bucher, K. & Hauri, H.-P. (1990) *Cell* **60,** 429–437.
9. Lisanti, M. P., Sargiacomo, M., Graeve, L., Saltiel, A. R. & Rodriguez-Boulan, E. (1988) *Proc. Natl. Acad. Sci. USA* **85,** 9557–9561.
10. Lisanti, M. P., Le Bivic, A., Saltiel, A. R. & Rodriguez-Boulan, E. (1990) *J. Membr. Biol.* **113,** 155–167.
11. Lisanti, M. P., Caras, I. W., Davitz, M. A. & Rodriguez-Boulan, E. (1989) *J. Cell Biol.* **109,** 2145–2156.
12. Powell, S. & Rodriguez-Boulan, E. (1989) *J. Cell Biol.* **109,** 296a (abstr.).
13. Brown, D. A., Crise, B. & Rose, J. K. (1989) *Science* **245,** 1499–1501.
14. Wilson, J. M., Fasel, N. & Kraehenbuhl, J.-P. (1990) *J. Cell Sci.* **96,** 143–149.
15. Low, M. & Saltiel, A. R. (1988) *Science* **239,** 268–275.
16. Lisanti, M. P., Rodriguez-Boulan, E. & Saltiel, A. R. (1990) *J. Membr. Biol.* **117,** 1–10.
17. Lisanti, M. P. & Rodriguez-Boulan, E. (1990) *Trends Biochem. Sci.* **15,** 113–118.
18. Caras, I. W., Weddell, G. N., Davitz, M. A., Nussenzweig, V. & Martin, D. W. (1987) *Science* **238,** 1280–1283.
19. Sargiacomo, M., Lisanti, M. P., Graeve, L., Le Bivic, A. & Rodriguez-Boulan, E. (1989) *J. Membr. Biol.* **107,** 277–286.
20. Thompson, J. A., Lau, A. L. & Cunningham, D. D. (1987) *Biochemistry* **26,** 743–750.
21. Griepp, E. B., Dolan, W. J., Robbins, E. S. & Sabatini, D. D. (1983) *J. Cell Biol.* **96,** 693–702.
22. Urban, J., Parczyk, K., Leutz, A., Kayne, M. & Kondor-Koch, C. (1987) *J. Cell Biol.* **105,** 2735–2743.
23. Bretscher, M. S. (1989) *EMBO J.* **8,** 1341–1348.
24. Graeve, L., Drikamer, K. & Rodriguez-Boulan, E. (1989) *J. Cell Biol.* **109,** 2809–2816.
25. Vega-Salas, D. E., Salas, P. J. I., Gundersen, D. & Rodriguez-Boulan, E. (1987) *J. Cell Biol.* **104,** 905–916.
26. Reggio, H., Webster, P. & Louvard, D. (1983) *Methods Enzymol.* **98,** 379–395.
27. Bacallao, R., Bomsel, M., Stelzer, E. H. K. & De May, J. (1989) *Methods Cell Biol.* **31,** 437–452.
28. Bangs, J. D., Andrews, N. W., Hart, G. W. & Englund, P. T. (1986) *J. Cell Biol.* **103,** 255–263.
29. Griffiths, G., Fuller, S. D., Back, R., Hollinshead, M., Pfeiffer, S. & Simons, K. (1989) *J. Cell Biol.* **108,** 277–297.
30. Green, R., Meiss, H. K. & Rodriguez-Boulan, E. (1981) *J. Cell Biol.* **89,** 230–239.
31. Simons, K. & van Meer, G. (1988) *Biochemistry* **27,** 6197–6202.
32. Parton, R. G., Prydz, C., Bomsel, M., Simons, K. & Griffiths, G. (1989) *J. Cell Biol.* **109,** 3259–3272.
33. Rothberg, K. G., Ying, Y., Kolhouse, J. F., Kamen, B. A. & Anderson, R. G. W. (1990) *J. Cell Biol.* **110,** 637–649.
34. van Meer, G., Gumbiner, B. & Simons, K. (1986) *Nature (London)* **322,** 639–641.
35. Montesano, R., Roth, J., Robert, A. & Orci, L. (1982) *Nature (London)* **296,** 651–653.